Biochimica et Biophysica Acta 1798 (2010) 1338–1347

Contents lists available at ScienceDirect

Biochimica et Biophysica Acta

journal homepage: www.elsevier.com/locate/bbamem

Vesicles with charged domains

Cíntia C. Vequi-Suplicy [a], Karin A. Riske [b], Roland L. Knorr [c], Rumiana Dimova [c,*]

[a] Instituto de Física, Universidade de São Paulo, CP 66318 CEP 05315-970, São Paulo, Brazil
[b] Departamento de Biofísica, Universidade Federal de São Paulo, R. Botucatu, 862 CEP 04023-062 São Paulo, Brazil
[c] Max Planck Institute of Colloids and Interfaces, Science Park Golm, 14424 Potsdam, Germany

ARTICLE INFO

Article history:
Received 17 August 2009
Received in revised form 15 December 2009
Accepted 22 December 2009
Available online 4 January 2010

Keywords:
Giant vesicle
Confocal microscopy
Phase separation
Lipid raft
Membrane domain
Charged lipid
DOPG
Egg sphingomyelin
DOTAP

ABSTRACT

This work summarizes results obtained on membranes composed of the ternary mixture dioleoylphosphatidylglycerol (DOPG), egg sphingomyelin (eSM) and cholesterol (Chol). The membrane phase state as a function of composition is characterized from data collected with fluorescence microscopy on giant unilamellar vesicles. The results suggest that the presence of the charged DOPG significantly decreases the composition region of coexistence of liquid ordered and liquid disordered phases as compared to that in the ternary mixture of dioleoylphosphatidycholine, sphingomyelin and cholesterol. The addition of calcium chloride to DOPG:eSM:Chol vesicles, and to a lesser extent the addition of sodium chloride, leads to the stabilization of the two-phase coexistence region, which is expressed in an increase in the miscibility temperature. On the other hand, addition of the chelating agent EDTA has the opposite effect, suggesting that impurities of divalent cations in preparations of giant vesicles contribute to the stabilization of charged domains. We also explore the behavior of these membranes in the presence of extruded unilamellar vesicles made of the positively charged lipid dioleoyltrimethylammoniumpropane (DOTAP). The latter can induce domain formation in DOPG:eSM:Chol vesicles with initial composition in the one-phase region.

1. Introduction

In the last years, the outburst of studies on multicomponent model membranes has been gradually shaping our understanding about cell membranes. The emerging concept pictures them as heterogeneous patchworks of groups of lipids, cholesterol and integral proteins [1]. The role of lipids in membrane structure and organization has received increased attention. In particular, the so-called lipid rafts are thought to be involved in several biological processes, such as signaling, membrane traffic, fusion and fission, apoptosis, cytoskeleton organization and adhesion [2–5]. Lipid rafts are nanometer-scale membrane domains rich in saturated lipids, cholesterol and specific proteins [6]. Their existence and role in cell membranes are still controversial, due to difficulties in resolving them in vivo.

The lipid fraction in cell membranes includes a surprisingly wide spectrum of lipid species and the reason for this diversity is not at all clear [7,8]. To further add to the compositional complexity, the lipids are asymmetrically distributed between the two membrane leaflets. Yet, to understand the membrane behavior when certain sterols or lipids are added or removed, e.g. during lipid hydrolysis, it is useful to start with examining the phase diagrams of symmetric model membranes with simpler composition [9].

In model lipid systems like vesicles or supported bilayers, phase separation in three component membranes made of a high- and a low-melting temperature lipids and cholesterol, has been reported for different lipid species and sterols. Giant unilamellar vesicles (GUVs) as a model system [10,11] present a powerful tool for mapping compositional phase diagrams [12–15], characterizing physical properties like fluidity (diffusion coefficients) [16], domain line tension [17–19], locating tie lines and miscibility critical points [20,21].

Both the raft domains and their surrounding lipid environment are fluid [22]. Thus, of special interest in the phase diagrams of ternary lipid mixtures is the two-phase region of coexistence of a liquid ordered (L_o) or raft phase, rich in the high-melting temperature lipid (saturated), and liquid disordered (L_d) phase, rich in the low-melting temperature lipid (typically unsaturated). Fluorescence microscopy of giant unilamellar vesicles allows for direct visualization of phase separation in the micrometer scale, taking advantage of the preferential partitioning of certain fluorescent dyes into one of the phases [23].

In the plasma membrane, the typical lipid composition leading to immiscibility of liquid phases is found mainly in the external bilayer leaflet, rich in phosphatidylcholines (PCs) with unsaturated chains and sphingomyelins (SMs). Cholesterol (Chol) is found in similar amount in both leaflets because of its fast flip–flop rate. Thus, lipid rafts are believed to form in the external leaflet. Studies on the phase behavior and coupling (or registering) of rafts in asymmetric lipid bilayers [24] show that the formation of domains in one bilayer leaflet composed of the classical raft mixture PC:SM:Chol induces domain

* Corresponding author. Tel.: +49 331 567 9615; fax: +49 331 567 9612.
E-mail address: dimova@mpikg.mpg.de (R. Dimova).

0005-2736/$ – see front matter © 2010 Elsevier B.V. All rights reserved.
doi:10.1016/j.bbamem.2009.12.023

formation on the other monolayer, rich in phosphatidylethanolamine (PE) and phosphatidylserine (PS). The latter is an anionic phospholipid found in the plasma membrane side facing the cytosol. Thus, formation of rafts on the external side of the cell membrane could be coupled to the formation of domains rich in the negatively charged lipid in the membrane leaflet facing the cytosol. Studies testing the ability of membranes containing charged lipids to form domains on their own are scarce [25] (note that earlier studies on binary mixtures containing charged lipids report domain formation induced by agents like polylysine and calcium ions [26,27]). Charged domains could influence the binding of oppositely charged proteins and ions present in the cytosol.

Here, we investigate the phase behavior of mixtures of the anionic phospholipid dioleoylphosphatidylglycerol (DOPG), egg sphingomyelin (eSM), and cholesterol. We used fluorescence microscopy to obtain an insight on the membrane phase state. To the best of our knowledge, this is the first report characterizing vesicles with charged PG-rich domains.

Our choice for the charged lipid is based on the fact that PCs and PGs bearing the same acyl chains show very similar thermal behavior,[1] e.g. almost identical temperatures of the main phase transition [30,31], which is not the case for PCs and PSs with identical acyl chains. Thus, we chose to replace the commonly used DOPC with its charged analog DOPG, because the effects of headgroup charges on the phase behavior of such mixtures could be recognized more easily. Furthermore, some studies reporting phase diagrams of membranes composed of ternary mixtures (see e.g. [15]) are based on vesicles prepared according to the method of Akashi et al. [32]. This method involves the use of PGs as an additional membrane component of up to 10–20 mol%. Such amounts of charged lipid were recently reported to have an effect on the domain morphology in vesicles made of dipalmitoylphosphatidylcholine (DPPC) and dilauroylphosphatidylcholine and DOPC [33]. Thus, the presence of the charged PG is expected to have a significant influence on the phase behavior of the composite PG:SM:Chol membranes.

We locate the region of two-phase L_d/L_o coexistence and study the stability of domains in this region with temperature and in the presence of ions. The addition of salt to DOPG membranes is known to decrease the lipid diffusion coefficient and the permeability to water [34]. These effects were interpreted as due to an increased lipid packing because of screening of the repulsion between the headgroup charges upon interaction with sodium and calcium ions [34]. Calcium ions bind to both neutral and negatively charged membranes [35] and at millimolar concentrations have condensation effect inducing area shrinkage of the membrane by several percents [35–38]. The interaction is strong and characterized by a 1:1 association constant of calcium ions with PG in the range 8.5–100 M^{-1} [39–41]. Our observations show that calcium ions can influence the stability of the fluid domains in DOPG:eSM:Chol vesicles.

Phosphatidylglycerols are found in membranes of prokaryotes and are widely used in studies on model membranes, particularly when interactions with positively charged molecules are investigated. In this way, one can mimic interactions of biologically relevant cationic macromolecules (e.g. peptides, protein domains, and hormones) with negatively charged membranes of microorganisms or cell membranes facing the cytosol. We exposed the negatively charged DOPG:eSM:Chol vesicles to positively charged liposomes made of dioleoyltrimethylammoniumpropane (DOTAP). DOTAP membranes have been studied most extensively for DNA delivery; see e.g. [42,43]. When present in membranes of saturated lipids like DPPC, DOTAP is known to significantly perturb the interfacial region of the membrane in addition to decreasing the melting temperature and broadening the phase transition [44,45]. Interestingly, when injected in the vicinity of homogeneous giant DOPG:eSM:Chol vesicles in the L_d phase, extruded DOTAP liposomes induce domain formation. The interaction may involve membrane fusion since oppositely charged vesicles, containing either DOTAP and/or PG, are known to adhere and fuse [46–48].

2. Materials and methods

2.1. Materials

The lipids DOPG (1,2-dioleoyl-*sn*-glycero-3-phospho-[1′-*rac*-glycerol], sodium salt), egg sphingomyelin, cholesterol and DOTAP (1,2-dioleoyl-3-trimethylammonium-propane, chloride salt) were purchased from Avanti Polar Lipids (Alabaster, AL) and Sigma (Steinheim, Germany). The chemical structures of cholesterol, palmitoyl-SM (the major component of eSM), DOPG, and DOTAP are given in Fig. 1. The fluorescent label $DiIC_{18}$ (1,1′-dioctadecyl-3,3,3′,3′-tetramethylindocarbocyanine perchlorate) was obtained from Molecular Probes (Eugene, OR) and perylene was purchased from Sigma. The chelating agent EDTA (ethylenediaminetetraacetic acid disodium salt dehydrate) was obtained from Sigma.

2.2. Methods

2.2.1. Preparation of giant DOPG:eSM:Chol unilamellar vesicles

Giant unilamellar vesicles (GUVs) were prepared by electroformation [49]. Briefly, ~12 µl of a 2 mg/ml lipid chloroform solution with the desired DOPG:eSM:Chol composition was spread on the surfaces of two conductive glasses coated with indium or fluor tin oxide. The lipid solution contained up to 0.5 mol% of the fluorescent dye $DiIC_{18}$, which is known to preferentially reside in the liquid disordered phase. Since $DiIC_{18}$ is positively charged, its preference to the DOPG-rich domains could be enhanced. Occasionally, we also introduced 0.3 mol% perylene in the mixtures. Perylene is typically excluded from solid domains. The dye concentrations are given with respect to the total lipid content in the solutions. The glasses were kept under vacuum for about 2 h to remove all traces of organic solvent. Then, they were placed with their conductive sides facing each other and separated by a 2 mm thick Teflon frame. The chamber was filled with 0.2 M sucrose solution and placed inside an oven at 60 °C. The glass plates were connected to a function generator and an alternating current of 1 V with a 10 Hz frequency was applied for 2 h. After that, the chamber was removed from the oven and allowed to cool to room temperature.

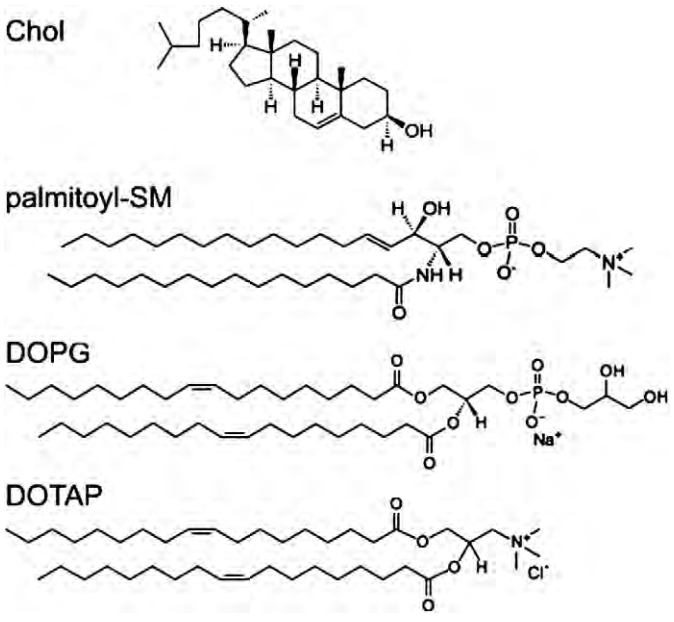

Fig. 1. Chemical structures of the membrane components used: cholesterol, palmitoyl-SM — the major component of eSM, DOPG, and DOTAP.

[1] Note that this is not necessarily the case for short-tailed lipids especially at low ionic strength; see e.g. [28,29].

Generally, the GUVs were observed few hours after preparation or in the following day, because this allowed for a longer equilibration time and consequently more vesicles had completed the phase separation process. The vesicles were diluted with 0.2 M glucose solution, which created a sugar asymmetry between the interior and the exterior of the vesicles. The osmolarities of the sucrose and glucose solutions were measured with a cryoscopic osmometer Osmomat 030 (Gonotec, Germany) and carefully matched to avoid osmotic pressure effects. In some of the experiments 0.1–0.2 mM EDTA, 1–10 mM NaCl or 0.5 mM $CaCl_2$ were added either to both the sucrose and the glucose solutions or only to the glucose solution.

2.2.2. Preparation of large unilamellar vesicles

Films of DOTAP or DOPG:eSM:Chol mixture were prepared from chloroform solutions of the lipids in glass tubes. The DOTAP solutions used for preparation of vesicles for microscopy observations contained 1 mol% $DiIC_{18}$. The tubes were placed under vacuum for about 2 h. A solution of 0.2 M glucose was added to obtain lipid concentration of 1 mM and the samples were vortexed for 1 min. The vesicle dispersion was extruded many times (>10) through polycarbonate pores of 200 and 100 nm diameter size, consecutively, using a miniextruder from Avanti Polar Lipids (Alabaster, AL), yielding large unilamellar vesicles (LUVs) of approximately 100 nm diameter as measured via dynamic light scattering.

2.2.3. Zeta-potential and dynamic light scattering measurements

Electrophoretic mobilities and size distribution of the extruded vesicles were determined at 21 °C with a Zetasizer Nano ZS (Malvern Instruments, Worcestershire, UK) operating with a 4 mW HeNe laser (632.8 nm), a detector positioned at the scattering angle of 173° and a temperature-control jacket for the cuvette. Each sample was degassed for 8 min to remove air bubbles. The cuvette was sealed to avoid evaporation and left for 3 min for temperature equilibration. Three dynamic light scattering measurements consisting of up to 50 consecutive runs of duration of 10 s were performed for each sample. Dynamic correlation functions were fitted by a second-order cumulant method to obtain the size distributions. Note that the quantitative interpretation of the DLS data depends on the applied fitting model. Here, the measurements were used to detect general trends in the evolution of the vesicle size distribution. For the zeta-potential measurements, the samples with volume 0.75 ml were loaded in folded capillary zeta-potential cells with integral gold electrodes. Three measurements consisting of 100 runs with duration 10 s were performed for every sample. The mobility u was converted to zeta-potential, ζ, using the Helmholtz–Smoluchowski relation $\zeta = u\eta/\varepsilon\varepsilon_0$, where η is the solution viscosity; ε, the dielectric constant of the solution and ε_0, the permittivity of free space. The standard deviation is about ± 3 mV. The viscosity of the glucose solution was taken into account in the analyses of the data obtained with both techniques.

2.2.4. Optical microscopy observation

The GUV solution was placed in a home-built observation chamber with a temperature-control jacket connected to a water circulating bath (Lauda RE-106, Westbury, NY). Due to the differences in density and refractive index between the sucrose and glucose solutions, the vesicles were stabilized by gravity at the bottom of the chamber and had better contrast when observed with phase contrast microscopy. For the conventional microscopy images, the vesicles were observed with an inverted microscope (Zeiss Axiovert 200, Jena, Germany) equipped with a Plan Neo-Fluar 63× Ph2 objective (NA 0.75). A set of filters with excitation at 540–552 nm and emission band of 575–640 nm (Zeiss filter set 20) and a mercury lamp HBO 100 W were used for observing vesicles labeled with $DiIC_{18}$. Image sequences were recorded with HSm digital camera (Zeiss, Jena, Germany) mounted on the microscope. The confocal images were taken on confocal microscope DM IRE2 (SP5 system, Leica Microsystems Heidelberg GmbH, Germany) equipped with a 40× HCX Plan APO objective (NA 0.75). A laser source at 561 nm was used to excite $DiIC_{18}$, and the 458 nm line was used for the excitation of perylene. To reduce artifacts due to light-induced domain formation [50,51] illumination with lower intensity was used. If domain sizes in vesicles were observed to grow (not due to coalescence of domains), the data was discarded.

Injection of 1 mM DOTAP LUVs close to DOPG:eSM:Chol GUVs was done with a glass micropipette (diameter 10–20 µm) controlled by a micromanipulator MP-225 from Sutter Instruments (Novato, CA). The micropipettes were pulled with PC-10 Puller from Narishige (Tokio, Japan). The injection flux was controlled manually with a micrometer knob pressing a 10 µl Hamilton syringe (Sutter Instruments, Novato, CA).

3. Results and discussion

We first describe our microscopy observations to characterize the overall phase behavior of DOPG:eSM:Chol membranes with various compositions. Our main goal was to locate the region of coexistence of the liquid disordered and liquid ordered phases, L_d/L_o. Then, we consider the effect of salt concentration and presence of divalent ions on the thermal stability of the fluid domains. We close with observations on DOPG:eSM:Chol vesicles in whose proximity we inject oppositely charged small extruded liposomes.

3.1. Phase behavior of DOPG:eSM:Chol membranes

We study the ternary mixture of eSM, DOPG and cholesterol using GUVs observed with confocal and conventional fluorescence microscopy. The formation of micron-size domains following demixing can be visualized on the surface of GUVs with fluorescently labeled lipids. The fluorescence dyes are homogeneously distributed in single-phase membranes, but are preferentially excluded from the phase whose structure is more disrupted by their inclusion [13,52–54]. Typically, this is the more ordered phase. Fluid domains in a fluid environment can be recognized by their smooth boundaries. Their shapes are typically round, but this depends on the line tension of the domains. Since the fluorescent dye $DiIC_{18}$ is predominantly excluded from the L_o phase, these domains appear dark. Solid domains can be recognized by sharp or angular features. Both of the fluorescent dyes used here ($DiIC_{18}$ and perylene) are excluded from such domains. The domains observed on the surface of a vesicle could be clearly distinguished from small vesicles in the interior when adjusting the focus to be midway through the giant vesicle.

At high temperatures, the vesicles prepared from ternary mixtures are homogeneous and fluid, and in the L_d phase. At room temperature, eSM is in the gel or solid (S_o) phase, whereas DOPG is in the fluid state already above −18 °C [31]. Thus, vesicles at room temperature can display immiscibility of phases depending on the specific composition.

Before we consider the phase diagram of DOPG:eSM:Chol, let us note that this is a quasi-ternary mixture. Egg sphingomyelin is a natural SM mixture highly enriched in long-chain saturated fatty acids, particularly in 16:0 (83.9%), and contains only small amounts of unsaturated ones (2–3% of 24:1). It exhibits a high melting temperature around 39 °C [55] showing an unusually cooperative phase transition (in contrast to brain SM), which arises from the fact that it contains primarily even-chain saturated fatty acids. Thus, the major sharp peak in the eSM exotherm is mainly associated with the chain-melting phase transition of palmitoyl-SM [56].

To study the DOPG:eSM:Chol membrane phase behavior, around 40 different compositions were explored. The compositions yielding vesicles with domains were examined with at least 3 preparations. Isolated vesicles that were larger than 10 µm in diameter and exhibited little or no defects (like lipid lumps or membrane tubes) were chosen. A typical GUV preparation contained around 30% of such vesicles. In order to achieve a more homogenous phase behavior for

each mixture, the GUVs were left to equilibrate at room temperature for several hours after preparation and before observation.

Some regions of the phase diagram were not accessible, either because the electroformation method resulted in poor yield of GUVs, or because cholesterol did not fully incorporate in the membrane during the vesicle preparation at high mole fractions. The solubility limits of cholesterol in PC membranes was found to be 66 mol% [57] and in ethanolamine membranes 51 mol% [58]. Above these solubility limits, cholesterol precipitates as crystals of cholesterol monohydrate. Thus, we did not examine vesicle compositions with molar fraction of cholesterol in this region.

We first consider the sides of the Gibbs triangle of the DOPG:eSM:Chol membranes, i.e. the binary mixtures of eSM and Chol, DOPG and Chol, and DOPG and eSM.

Addition of cholesterol (up to about 10 mol%) is known to cause a slight decrease in the temperature of the transition peak of eSM followed by a modest increase at higher cholesterol concentrations [55]. At cholesterol fractions above about 30 mol%, the eSM:Chol membranes at room temperature are in the L_o state [59], while at cholesterol fractions between approximately 8 mol% and 20–30%, evidence for L_o/S_o coexistence in palmitoyl-SM:Chol membranes is provided from differential scanning calorimetry [60,61] and fluorescence quenching studies [62]. Thus, between these limits, we expected to find vesicles with coexisting S_o and L_o domains. However, we did not detect such coexistence region in our fluorescence microscopy observations on giant eSM:Chol vesicles, similarly to results obtained with palmitoyl-SM:Chol mixtures [63]. For the composition eSM:Chol 9:1 (molar ratios), the vesicles were homogeneously fluorescent, with facets typical for gel-like membranes, and exhibited no thermal shape fluctuations of the vesicles. The next examined mixtures 8:2, 7:3 and 6:4 appeared also homogenous but with detectable fluctuations, which is why we assume that they belong to the L_o phase. No domains were observed. A possible explanation could be that solid domains are not distinguished because they are smaller than 1 μm. This is consistent with NMR results showing small (<1 μm) domains in membranes with coexisting S_o/L_o phases [64].

Following our protocol for vesicle electroformation, vesicles prepared from the binary mixture DOPG:Chol were with very low yield for reporting representative results. However, the phase behavior of this binary mixture is not rich. The DOPG:Chol membranes are expected to be in L_d phase, which continuously changes to L_o phase with increasing the cholesterol fraction. This change mainly leads to an increase in the packing order as reflected by the lower permeability of the bilayers to water [65].

For vesicles made of DOPG and eSM, one expects a region of coexistence of fluid and gel phases. For the studied compositions, we observe that this immiscibility region is broader compared to that observed in other mixtures of low- and high-melting temperature lipids like eSM and palmitoyloleoylphochatidylcholine (POPC) or eSM and DOPC. Vesicles with composition DOPG:eSM in the broad range from 8:2 to 2:8 show domains, suggesting that DOPG and eSM mix poorly. Vesicles with composition DOPG:eSM 1:9 appeared with homogeneous fluorescence but rigid and with faceted shapes indicating that they are in the S_o phase.

To describe our observations on vesicles from the quasi-ternary DOPG:eSM:Chol mixture, we first consider the composition 1:1:1. At room temperature, vesicles made of the same fractional composition but of DOPC:eSM:Chol mixture, also known as the "canonical" raft mixture, exhibit liquid domains and the miscibility temperature of this mixture was reported to be 41–43 °C [14]. Replacing DOPC by DOPG has a significant consequence: At room temperature, vesicles prepared from this mixture are homogeneous and in the one-phase state. Phase separation was not observed even down to ~16 °C (lower temperatures could not be explored with our setup), showing that the presence of the charged lipids leads to depression of the miscibility temperature by more than 25 °C. We conclude that the repulsion among the charged headgroups in the DOPG-containing membranes hinders phase separation.

At about the same fraction of cholesterol (30 mol%) and arbitrary mole ratio between DOPG and eSM we still do not observe any domain formation in contrast to the phase behavior of DOPC:SM:Chol membranes [63]. Presumably, less cholesterol is needed to mix DOPG with eSM at room temperature as compared to DOPC with SM.

The results for all of the explored mixtures of DOPG:eSM:Chol at room temperature are summarized in Fig. 2. We classified the vesicles in four categories: i) homogeneous and with fluid membrane as visible from the thermal fluctuations, e.g. belonging to either L_o or L_d phase (solid red circles); ii) homogenous but without thermal fluctuations, i.e. gel-like (solid black squares); iii) with round fluid domains in fluid environment, i.e. representing the L_d/L_o coexistence region (red semi-filled circles); and iv) with non-round but angular or worm-like domains corresponding to either L_d/S_o or L_o/S_o or $L_d/L_o/S_o$ coexistence (black semi-filled squares). Note that our observations were done on vesicles prepared in sucrose and subsequently diluted in glucose. The phase behavior of the membranes in pure water or various buffers may differ slightly.

For the region of low cholesterol content (<20 mol%) and small fractions of eSM, we observe solid structures with hexagonal-like symmetry; see the vesicle snapshot for the 7:2:1 mixture in Fig. 2. Upon increasing the fraction of eSM, angular shapes and worm-like domains are detected; see the snapshots at the bottom in Fig. 2.

We attempted to locate the region of coexistence of L_o and L_d phases at room temperature. Compositions from this region are indicated with round semi-filled symbols in the graph in Fig. 2. Compared to the phase diagram of DOPC:SM:Chol [63,66,67], the size of the region of fluid phase immiscibility is significantly reduced when the zwitterionic lipid DOPC is replaced by the anionic lipid DOPG. The coexistence region is shifted towards the eSM corner of the triangle, i.e. to low DOPG and Chol content (≤30%). Indeed, some vesicles in these preparations (less than about 20%) were homogeneous and showed no domains. This suggests that the L_d/L_o region is relatively narrow and the examined vesicle compositions are close to the miscibility line. The borders of the charged domains showed significant fluctuations, even when the temperature was decreased to 18 °C, suggesting that either these membrane compositions are close to the critical point, or the line tension of DOPG-rich domains in DOPG:eSM:Chol mixtures is lower than that of DOPC-rich domains in the DOPC:eSM:Chol mixtures [14,20]. At room temperature, only three of the examined compositions appeared to belong to the L_d/L_o region: 3:5:2, 2:6:2 and 1:7:2. The mixture 4:4:2 is in the one-phase region but demixes to L_d/L_o domains already at 22 °C, suggesting that it is close to the boundary of the L_d/L_o coexistence region.

Note that the presence of as little as 10 mol% of PG (as in the mixture 1:7:2) influences the phase state of the membrane. This result should be considered when working with vesicles prepared by the method of "gentle hydration" [32], which involves the use of PGs of up to 20 mol%. This method for example has been used to determine the phase diagram of DOPC:distearoylphosphatidylcholine:Chol [15].

We are aware of existing discrepancies between phase diagrams measured by different methods [68]. Moreover, applying only one technique to characterize the phase diagram of multicomponent membranes is a restricted approach. Locating the exact phase boundaries for membranes made of the ternary mixture DOPG:eSM:Chol is rather complex. When addressing this task with fluorescence microscopy only, one encounters the following difficulties: First, there is always a slight variation in composition between different vesicles in a batch. This can lead to a variation in the measured transition temperatures. Second, for a fixed temperature, compositions close to the miscibility boundary can exhibit both homogeneous vesicles and such with phase separated domains. For the electroformation method for one vesicle preparation, Veatch and Keller [69] have estimated a variation of ±2 mol% cholesterol between individual vesicles. Judging from the area fraction of the domains in vesicles from one batch, our experience suggests that this spread may be even larger for certain compositions. For this reason, we

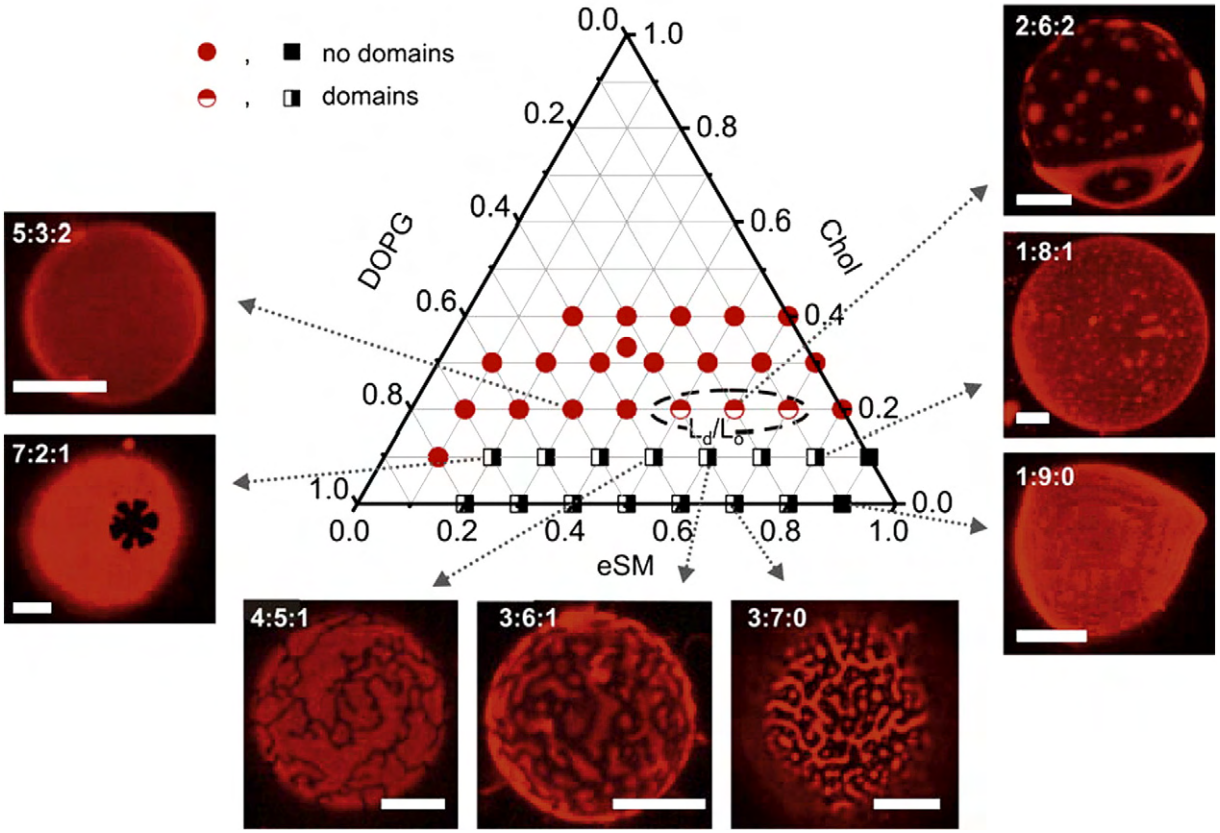

Fig. 2. Summary of microscopy observations on giant unilamellar vesicles made of DOPG:eSM:Chol at room temperature (~23 °C). The snapshots show typical confocal microscopy images (either 3D projection of half of a selected vesicle or a 2D scan with an open pinhole) of giant vesicles for each composition as indicated in the upper left corners of the images. The fluorescent dye used, $DiIC_{18}$, partitions preferentially into the liquid disordered phase. The filled symbols in the graph correspond to homogenous vesicles without domains, the semi-filled symbols correspond to vesicles with domains. The circles correspond to vesicles, which appear to be fluid and if domains are present they are round. The region of L_d/L_o phase coexistence is schematically indicated with the dashed line. The squares correspond to vesicles which appear to be solid (do not fluctuate and have facets) and if domains are present they are not round but have angular or worm-like shapes. All scale bars correspond to 10 μm.

varied the explored vesicle compositions in relatively large steps of 10 mol% of one of the components. We also examined large populations of vesicles. In addition, to circumvent possible influence of budding or curvature sorting on the membrane composition [70–73], we typically avoided using vesicles with inclusions and those externally connected to lipid lumps or clusters of smaller vesicles. Third, in composition regions where the domains are small, the domain shapes may be difficult to resolve and thus the conclusion about the observed phase may be subjective. Fourth, for areas in the phase diagram where the fraction of the fluid phase is very low, the fluorescent dye is concentrated in the small fluid domains and may influence the phase state of the lipids. Finally, we employed two fluorescent dyes ($DiIC_{18}$ is excluded from the L_o and S_o domains and perylene is typically excluded from the S_o domains). However, this did not help significantly to determine the different domain types. The phase of the observed domain could be inferred only from its shape if optically resolved.

Because of the above considerations, we refrained from attempts to draw the exact boundaries in the phase diagram but set the modest goal to mainly locate a region of coexistence of the two fluid phases L_d and L_o relevant for rafts in cell membranes. The presence of these phases in giant vesicles is typically evidenced by round domains.

We then studied the stability of the fluid domains in the L_d/L_o region with temperature. Of the three studied compositions, the mixture 3:5:2 has the highest miscibility temperature. Fig. 3 shows the behavior of such a vesicle with raising temperature: the fluctuations in the domain shapes become stronger, and the domains melt at 28 °C. This temperature is significantly lower as compared to that of the L_d/L_o coexistence region of the classical mixture with DOPC, which is stable up to ~41 °C [14]. The miscibility temperatures for the mixtures 2:6:2 and 1:7:2 DOPG:eSM:Chol were around 23–25 °C. Note that these temperatures lie well below the melting temperature of eSM (39 °C). We remind that the miscibility temperatures here are detected with fluorescence microscopy, which cannot resolve domains with sizes below the optical resolution limit, if they are present.

3.2. Stability of domains in the L_d/L_o region in the presence of different solutes

Lipids in different phases occupy different area. For example, the area of a lipid membrane increases upon melting. The melting temperatures of charged membranes are typically lower than those of neutral ones, since the charges on the headgroups repel each other, favoring the fluid state with larger area per lipid. Increasing the ionic strength screens the electrostatic interactions, thus playing a crucial role on the phase behavior of charged membranes. Furthermore, some ions can bind to the charged headgroups changing the bilayer material properties. The effect of ionic concentration on the stability of charged membrane domains is not straightforward to predict. The addition of salt is expected to screen possible repulsion between charged domains, thus allowing them to easily coarsen by coalescence. Moreover, high ionic strength and/or ion binding may have an effect on the lipid headgroups and packing in the bilayer presumably promoting the formation of domains rich in the charged lipid. In both cases, we expect that the phase separation process will be facilitated at higher ionic strengths, which should be associated with an increase in the miscibility temperature.

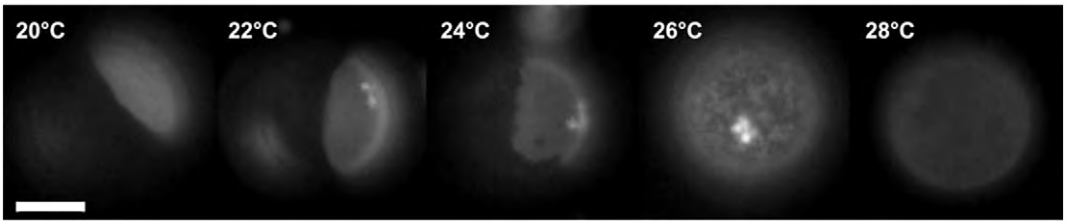

Fig. 3. A sequence of snapshots obtained with fluorescence microscopy on a GUV made of DOPG:eSM:Chol 3:5:2 showing the effect of temperature on domain stability. The vesicle was left to equilibrate for 5 min at each temperature. The scale bar corresponds to 10 μm.

The influence of the salts NaCl and $CaCl_2$ on the stability of DOPG-rich domains was studied for two mixtures, 3:5:2 and 2:6:2, which show L_d/L_o phase coexistence at room temperature. The miscibility temperatures were used to characterize the stability of the domains. Because we are aware of the presence of impurities of divalent cations in aqueous solutions [74,75], we first tested the effect of adding the chelating agent EDTA. The latter complexes free multivalent cations and is not expected to interact with the membranes. The lipid concentration in GUV samples is typically in the micromolar range. Thus, the presence of impurities at similar concentrations can affect the phase behavior of membranes, particularly charged ones [74]. For example, calcium is known to induce phase separation in black lipid membranes composed of PC:PG mixtures [76] and to increase the main phase transition temperature of PG membranes [74,77].

The miscibility temperatures measured for vesicles in the L_d/L_o coexistence region in the presence of different additives are summarized in Table 1. The addition of 0.1 mM EDTA decreased the miscibility temperature of vesicles in the L_d/L_o coexistence region by ~6 °C for the 3:5:2 mixture and by ~3 °C for the 2:6:2 mixture. This result indicates that divalent cations present as impurities stabilize charged domains in GUVs with stronger effect on the mixture with the larger fraction of DOPG. Further increasing the EDTA concentration to 0.2 mM did not lead to additional decrease in the miscibility temperature, suggesting that the concentration of impurities is below that complexed by 0.1 mM EDTA.

When 0.5 mM $CaCl_2$ was added to the vesicles (in the absence of EDTA), the miscibility temperature of the 2:6:2 mixture increased considerably (by ~5 °C) compared to the no-additive case. This confirms our conclusion based on the experiments with EDTA that charged domains are stabilized by the presence of divalent ions. Little or no effect was detected in the 3:5:2 mixture, which exhibited the highest miscibility temperature in the L_d/L_o coexistence region when no calcium was added. Higher concentrations of $CaCl_2$ (1–5 mM) increased the vesicle tension (the membrane fluctuations were suppressed), induced vesicle aggregation and adhesion to the cover slip followed by vesicle rupture. Similar effects were observed on giant vesicles containing PS in the presence of calcium ions [35], while the adsorption of divalent cations to charged monolayers was shown to decrease the area per molecule [37] and increase the surface tension [78,79], consistent with our observations.

Table 1
Miscibility temperatures of GUVs in the L_d/L_o coexistence region in the absence and presence of different solutes. Data for two different membrane compositions are given. The vesicles were prepared in sucrose and diluted in glucose solution containing the specified amount of additives as indicated. The case where no EDTA or salt was added to the sugar solutions is referred to as "no additive".

Solution	DOPG:eSM:Chol membranes	
	3:5:2	2:6:2
No additive	27–29 °C	23–25 °C
0.1–0.2 mM EDTA	21–22 °C	21–22 °C
0.5 mM $CaCl_2$	27–30 °C	27–30 °C
1–10 mM NaCl	27–30 °C	23–26 °C
1–10 mM NaCl + 0.1 mM EDTA	22–26 °C	22–27 °C

Addition of 1, 5 and 10 mM NaCl to vesicles in the absence of EDTA had little or no effect on the miscibility temperature. To avoid the influence of divalent ion impurities, the effect of NaCl was also examined in the presence of 0.1 mM EDTA. In the latter case, the addition of 1–10 mM NaCl induced a mild increase of the miscibility temperature of the domains as compared to the data obtained in the presence of EDTA only; see Table 1. Miscibility temperatures as high as those measured for the L_d/L_o region in DOPC:eSM:Chol mixtures [14] were not observed. This indicates that for the explored ionic strengths the charges in the membrane are only partially screened. Indeed, for other PG systems it has been shown that even 500 mM NaCl is insufficient to completely suppress the repulsion between adjacent bilayers [80]. Here we could not explore such high concentrations because already upon the addition of 10 mM NaCl a fraction of the vesicles ruptured. This suggests that monovalent ions might also induce tension on the membrane. When 50 mM NaCl was added, the majority of the vesicles adhered to the glass and ruptured.

Our experiments in the presence of different solutes were performed both on vesicles having the additives inside and outside and on vesicles where the solute was added only to the external solution. In the former case the vesicle yield was poorer. In both cases the vesicles behaved similarly indicating that the stabilization/melting of domains in the outer bilayer leaflet is coupled to domain formation/destabilization in the inner bilayer leaflet as shown for asymmetrical bilayer systems [24].

3.3. Interaction of DOPG:eSM:Chol GUVs with extruded cationic liposomes

Upon phase separation, vesicles with charged lipids acquire regions with higher surface charge density. In our case, these are the DOPG-rich domains. Negatively charged domains can act as recognition patches for positively charged molecules (e.g. positively charged peptides or protein domains) or particles. These positively charged molecules may adhere to the membrane or insert into the bilayer. In both cases, they are expected to change the phase behavior of multicomponent membranes. Here we studied the effect of injecting a dispersion of extruded large unilamellar vesicles (LUVs) made of the positively charged lipid DOTAP, in the vicinity of giant DOPG:eSM:Chol vesicles. We explored both homogeneous fluid GUVs and GUVs in the fluid two-phase L_d/L_o region.

We used a dispersion of 1 mM extruded DOTAP LUVs labeled with 1 mol% $DiIC_{18}$. The solution was injected with a glass pipette, which was held at a distance of about 50 μm away from the selected vesicle. The size and surface charge of the DOTAP vesicles are discussed further.

We studied the effect of injecting extruded DOTAP liposomes in the vicinity of two-phase L_d/L_o GUVs with composition 3:5:2. To ensure the domain stability, we worked at lower temperature, namely 18 °C. At this temperature DOTAP is fluid. It has a low melting temperature, similarly to DOPG because of the identical acyl chains, see Fig. 1.

We first used GUVs which were fluorescently labeled to be able to observe the area fraction and location of the DOPG-rich domains; see

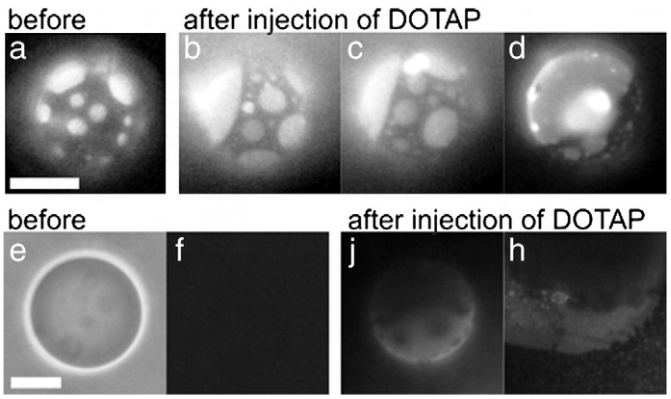

Fig. 4. Sequences of snapshots showing the effect of injection of a LUV dispersion of 1 mM DOTAP vesicles labeled with 1 mol% $DiIC_{18}$ in the vicinity of two GUVs made of 3:5:2 DOPG:eSM:Chol: a vesicle labeled with $DiIC_{18}$ (a–d), and a vesicle, which is not labeled (e–h). The experiments were performed at 18 °C. The snapshots were taken a few seconds apart. The scale bars correspond to 10 μm. Before injection of DOTAP vesicles (a), the GUV labeled with $DiIC_{18}$ exhibited domains. The bright background seen right after the injection (b) was due to the flow of fluorescently labeled DOTAP LUVs reaching the giant vesicle. A few seconds after injection (c, d), the area fraction of the fluorescently labeled L_d domains in the GUV increased. In less than a minute, the vesicle adhered to the cover slip and ruptured. Before injection of DOTAP, the unlabeled GUV could be observed under phase contrast (e) but not with fluorescence microscopy (f). Several seconds after injection of DOTAP LUVs from the lower right side, domains were observed to form on the GUV (j). After that, the vesicle adhered to the glass and ruptured, spreading on the substrate (h).

Fig. 4a. After injection, the positively charged DOTAP vesicles induced an increase in the area fraction of the L_d DOPG-rich domains; see Fig. 4b–d. The fluctuations in the domain boundaries decreased, suggesting an increase in the line tension and stabilization of the domains. Several seconds after the injection, brighter spots could be observed on the vesicle surface (Fig. 4c and d), indicating local condensation or formation of small buds. After a few tens of seconds, the vesicles typically adhered to the glass surface and ruptured (here not shown; an example with another vesicle is given in Fig. 4h). This is due to the tendency of the positively charged DOTAP to strongly adhere to the negatively charged glass surfaces. The GUVs adhesion in the presence of DOTAP is similar to that observed in the presence of calcium. The adhesion and rupture of the DOPG:eSM:Chol GUVs is an indication that, in the presence of extruded DOTAP vesicles, the overall surface charge of the GUVs changes from negative to positive leading also to adhesion to the negatively charged glass. The change in the surface charge is supported by zeta-potential measurements described further. Because the GUVs were unstable and ruptured in the presence of extruded DOTAP vesicles, we could not study the stability of the domains as a function of temperature. These experiments mainly demonstrate that DOTAP influences the phase state of the DOPG:eSM:Chol membranes.

We also explored the possibility to use fluorescent DOTAP vesicles as markers for the charged domains in a two-phase GUV, which was not labeled fluorescently. We expected that if DOTAP vesicles only adhere to the GUV, they would prefer the DOPG-rich domains and would fluorescently mark them. If the DOTAP vesicles fuse with the membrane of the GUV, complex behavior of the domains can be expected because of a change in the membrane composition. The images in Fig. 4e–h illustrate the results from these experiments. We first located a GUV under phase contrast (Fig. 4e). A few seconds after injecting the fluorescently labeled DOTAP vesicles, we observed fluorescence from domains on the GUV surface. It appeared that in this case, the continuous phase was L_d (fluorescent) surrounding smaller L_o domains (Fig. 4j), while in vesicles of this composition in the absence of DOTAP the continuous phase is typically L_o; see Fig. 4a. The domain repartitioning implies a change in the GUV membrane composition. Presumably this is due to fusion of DOTAP vesicles with the GUV. However, we did not detect an increase in the size of the inspected giant vesicles. Similarly to the vesicle described in Fig. 4a–d, this GUV also adhered to the glass surface and ruptured coating the substrate with a bilayer with a fluorescent pattern; see Fig. 4h. Adhesion affects the entropy of the membrane by dampening its thermal undulations and has been shown to induce phase segregation in adhesion zones between vesicles or vesicles and a substrate [81]. However, here the vesicles were observed to phase separate already before adhering to the glass surface.

We then explored the effect of injecting extruded DOTAP vesicles in the vicinity of labeled GUVs in the fluid one-phase region. Fig. 5 shows the result on a GUV with the composition 4:4:2. This membrane composition belongs to the one-phase region but is close to the miscibility boundary of the L_d/L_o region; see Fig. 2. After initiating the injection, we detect local domain formation at the vesicle side facing the injection pipette (lower right side). This side of the vesicle is exposed to higher concentration of DOTAP, which locally influences the phase state of the membrane via adsorption or fusion. The bright DOPG-rich L_d domain formed there presumably depletes the surrounding from DOPG, leading to the formation of relatively large L_o domains (Fig. 5, snapshots at 75–121 s). After a couple of minutes, the L_o domains decrease in size (Fig. 5, 148–176 s). Note that after the DOTAP injection is terminated, the local concentration of LUVs decreases due to diffusion.

The sequence of events shown in Figs. 4 and 5 is rather complex to provide a thorough explanation, as the membrane composition might be changing depending on the amount of DOTAP inserting into the bilayer via fusion. Furthermore, an equilibrium state is hardly ever reached, because the vesicles usually rupture after several seconds

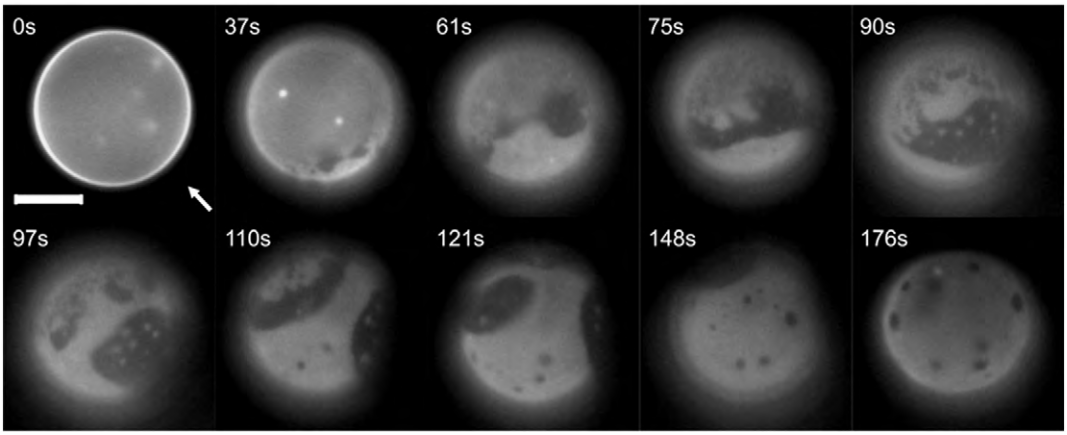

Fig. 5. Sequence of snapshots presenting the effect of injecting dispersion of 1 mM DOTAP LUVs labeled with 1 mol% $DiIC_{18}$ in the vicinity of a GUV made of DOPG:eSM:Chol 4:4:2. The time after injection is indicated in the upper left corner of each snapshot. The arrow in the first snapshot shows the direction of injection. The scale bar corresponds to 10 μm.

due to adhesion to the cover slip. Suitably coating the glass walls of the working chamber might provide a solution to this problem. Control on the local concentration of DOTAP should also be pursued. However, the purpose of these experiments was to demonstrate that interaction with positively charged small vesicles changes the phase behavior of the ternary mixture DOPG:eSM:Chol. Using individual and better suited fluorescent labels on each of the membrane types might help for quantitative characterization of the interaction of the DOTAP vesicles with the GUVs and to clarify whether membrane adhesion or fusion is the main process involved. Efforts in this direction will be subject of future work.

To complement our microscopy observations on the interaction of the DOPG:eSM:Chol GUVs with the extruded DOTAP vesicles and to attempt to find out whether the interaction between them occurs mainly via adhesion or fusion, zeta-potential and dynamic light scattering (DLS) measurements were performed. Because both experimental techniques are limited to particles whose size is not larger than a couple of micrometers, we used extruded and not giant DOPG:eSM:Chol vesicles. Only the homogeneous 4:4:2 mixture was investigated. The DLS data showed that on the average the extruded DOTAP vesicles had a mean diameter around 105 nm and positive zeta-potential of +85 mV, while the DOPG:eSM:Chol vesicles were slightly larger with diameters around 130 nm and with negative zeta-potential with average value of −70 mV. A few minutes after mixing the two vesicles dispersion in 1:1 ratio, the size distribution in the measuring cell drastically changed giving rise to an additional population of particles with diameters around 0.5 μm and much broader distribution in the following hours; see Fig. 6a. Immediately after mixing, only a single peak in the zeta-potential measurements was detected around +50 mV. In the next several hours it gradually shifted to +64 mV. Thus, upon mixing, the DOPG:eSM:Chol vesicles, which are initially negatively charged, change their surface charge to positive. Indeed, the data indicates approximately proportional compensation of positive and negative charges considering the molar concentrations of DOTAP and DOPG, respectively. The DLS data shows that the vesicle sizes increase. This can be both due to aggregation induced by adhesion of the oppositely charged vesicles or due to their fusion. Visual inspection of the mixed vesicle dispersion after the measurements did not show increase in turbidity or precipitation. We investigated this dispersion with phase contrast microscopy and found a small fraction of giant vesicles with diameters of up to around 40 μm a few hours after mixing the solutions; see Fig. 6b and c. No such vesicles were found in dispersions of extruded DOTAP or DOPG:eSM:Chol 4:4:2 vesicles when left to equilibrate for a few hours. The background texture in Fig. 6c shows that the majority of the vesicles are still sub-microscopic.

The presence of giant vesicles in the mixture suggests that the interaction between the two types of liposomes involves membrane fusion, although adhesion is likely to occur prior to fusion. We did not observe an increase in the size of the giant vesicles made of DOPG:eSM:Chol to which the extruded DOTAP vesicles were injected. A plausible explanation could be that the area change was too small to be detected or that DOTAP might have a condensation effect on DOPG:eSM:Chol membranes. Such condensation may lead to higher tension on the DOPG:eSM:Chol vesicles, which is known to facilitate fusion [82].

Upon fusion, the membrane of the resulting vesicles is a mixture of cationic, anionic and neutral lipids. Such mixtures have the propensity to form inverted nonlamellar phases when the mean surface charge approaches neutrality [83], and thus, are not expected to be stabilized as giant vesicles, which exemplify a system in the lamellar phase. However, we were not able to probe the stability of the DOPG:eSM:Chol vesicles after exposure to DOTAP dispersions, because the GUVs generally ruptured shortly after the DOTAP injection.

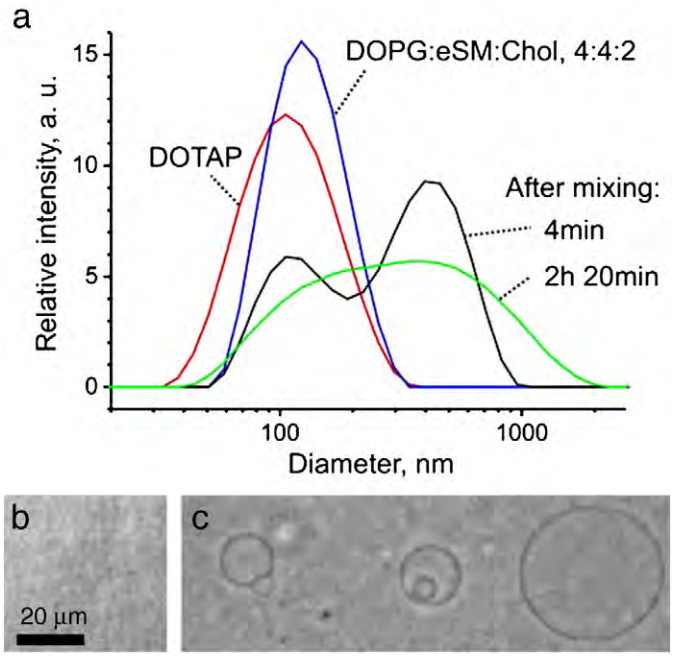

Fig. 6. DLS data from dispersions of extruded DOTAP and DOPG:eSM:Chol 4:4:2 vesicles and their mixture (a), and microscopy observations on these samples (b, c). The size distribution curves shift to larger diameters at a certain time after mixing as indicated in the graph (a). A snapshot of the dispersion of extruded vesicles made of DOTAP (b) shows the absence of particles resolvable with phase contrast microscopy; similar image is obtained from a dispersion of extruded vesicles made of DOPG:eSM:Chol 4:4:2. Snapshots recorded several hours after mixing of the two types of extruded vesicles show that giant vesicles with diameters of up to about 40 μm can be found (c).

4. Conclusions

We explored the phase diagram of the quasi-ternary mixture DOPG:eSM:Chol complementing the available literature on domain formation in neutral model membranes. To the best of our knowledge, this is the first study on the stability of fluid charged domains in giant vesicles. We show that the composition range leading to formation of rafts is significantly reduced when one of the lipids is charged. Addition of salt increases the stability of the domains, whereas the chelating agent EDTA has the opposite effect. Thus, ions like calcium in the solution have a stabilizing effect on the domains. Intracellular release of calcium, known to occur after cell stimulation, might be influencing the local phase state of the membranes.

Charged domains, here DOPG-rich, can act as recognition sites on the membrane for selective interaction with positively charged molecules or particles. Here, we demonstrated this possibility using a dispersion of DOTAP vesicles. The complex phase behavior observed in our experiments needs further exploration.

Studying negatively charged domains in model membranes is imposed by the overwhelming need for understanding the basic biophysics of raft formation in the plasma membrane. Even though rafts are believed to form in the external leaflet of the plasma membrane, evidence for registering of rafts in asymmetric lipid bilayers has been recently provided [24], justifying the need for studying phase separation in membranes with charged lipids. Negative charges in the lipid headgroup significantly increase the complexity of the system involving the interplay between electrostatic interactions and hydrophobic effects, in addition to inter-domain elastic interactions [84]. The need of studying phase separation in charged membranes is further motivated by the possible involvement of charged rafts in regulating protein activity in the cytosol which may either be governed by or may regulate the phase separation in the external leaflet of the plasma membrane.

Intracellular membranes are negatively charged and are close to a critical point [8,85]. Thus, proteins may easily influence their phase state locally, facilitating processes like budding and vesicular trafficking. Our study is only a scratch on the surface of a bulk of still unexplored knowledge required for understanding the versatile mechanisms, which cell membranes employ to function.

Acknowledgments

We thank the editor of this issue for the invitation to submit this article. We also thank C. Remde and M. Staykova for the support on the zeta-potential and microscopy measurements. R.D. thanks R. Lipowsky and C. Marques for the stimulating discussions. C.C.V.-S. thanks M. T. Lamy for allowing this new experience with GUVs. R.D. acknowledges the support of the German Research Foundation (Deutsche Forschungsgemeinschaft). K.A.R. and C.C.V.-S. acknowledge the support of Fundação de Amparo à Pesquisa do Estado de São Paulo (FAPESP). K.A.R. also acknowledges the financial support of INCT-FCx.

References

[1] D.M. Engelman, Membranes are more mosaic than fluid, Nature 438 (2005) 578–580.
[2] M. Edidin, The state of lipid rafts: from model membranes to cells, Annu. Rev. Biophys. Biomol. Struct. 32 (2003) 257–283.
[3] D. Holowka, J.A. Gosse, A.T. Hammond, X.M. Han, P. Sengupta, N.L. Smith, A. Wagenknecht-Wiesner, M. Wu, R.M. Young, B. Baird, Lipid segregation and IgE receptor signaling: a decade of progress, BBA-Mol. Cell Res. 1746 (2005) 252–259.
[4] J. Fullekrug, K. Simons, Lipid rafts and apical membrane traffic, Gastroenteropancreatic Neuroendocr. Tumor Dis.: Mol. Cell Biol. Asp. 1014 (2004) 164–169.
[5] D. Meder, M.J. Moreno, P. Verkade, W.L.C. Vaz, K. Simons, Phase coexistence and connectivity in the apical membrane of polarized epithelial cells, Proc. Natl. Acad. Sci. U. S. A. 103 (2006) 329–334.
[6] K. Simons, E. Ikonen, Functional rafts in cell membranes, Nature 387 (1997) 569–572.
[7] B.G. Gennis, Biomembranes: Molecular Structure and Function, Springer-Verlag, New York, 1989.
[8] G. van Meer, D.R. Voelker, G.W. Feigenson, Membrane lipids: where they are and how they behave, Nat. Rev. Mol. Cell Biol. 9 (2008) 112–124.
[9] G.W. Feigenson, Phase diagrams and lipid domains in multicomponent lipid bilayer mixtures, BBA-Biomembranes 1788 (2009) 47–52.
[10] P.L. Luisi, P. Walde, Giant Vesicles, John Wiley & Sons, Ltd, Chichester, 2000.
[11] R. Dimova, S. Aranda, N. Bezlyepkina, V. Nikolov, K.A. Riske, R. Lipowsky, A practical guide to giant vesicles. Probing the membrane nanoregime via optical microscopy, J. Phys.: Condens. Matter 18 (2006) S1151–S1176.
[12] C. Dietrich, L.A. Bagatolli, Z.N. Volovyk, N.L. Thompson, M. Levi, K. Jacobson, E. Gratton, Lipid rafts reconstituted in model membranes, Biophys. J. 80 (2001) 1417–1428.
[13] J. Korlach, P. Schwille, W.W. Webb, G.W. Feigenson, Characterization of lipid bilayer phases by confocal microscopy and fluorescence correlation spectroscopy, Proc. Natl. Acad. Sci. U. S. A. 96 (1999) 8461–8466.
[14] S.L. Veatch, S.L. Keller, Separation of liquid phases in giant vesicles of ternary mixtures of phospholipids and cholesterol, Biophys. J. 85 (2003) 3074–3083.
[15] J. Zhao, J. Wu, F.A. Heberle, T.T. Mills, P. Klawitter, G. Huang, G. Costanza, G.W. Feigenson, Phase studies of model biomembranes: complex behavior of DSPC/DOPC/cholesterol, BBA-Biomembranes 1768 (2007) 2764–2776.
[16] N. Kahya, D. Scherfeld, K. Bacia, B. Poolman, P. Schwille, Probing lipid mobility of raft-exhibiting model membranes by fluorescence correlation spectroscopy, J. Biol. Chem. 278 (2003) 28109–28115.
[17] A.J. Garcia-Saez, S. Chiantia, P. Schwille, Effect of line tension on the lateral organization of lipid membranes, J. Biol. Chem. 282 (2007).
[18] C. Esposito, A. Tian, S. Melamed, C. Johnson, S.Y. Tee, T. Baumgart, Flicker spectroscopy of thermal lipid bilayer domain boundary fluctuations, Biophys. J. 93 (2007) 3169–3181.
[19] A.W. Tian, C. Johnson, W. Wang, T. Baumgart, Line tension at fluid membrane domain boundaries measured by micropipette aspiration, Phys. Rev. Lett. 98 (2007) 208102.
[20] A.R. Honerkamp-Smith, S.L. Veatch, S.L. Keller, An introduction to critical points for biophysicists; observations of compositional heterogeneity in lipid membranes, BBA-Biomembranes 1788 (2009) 53–63.
[21] S.L. Veatch, K. Gawrisch, S.L. Keller, Closed-loop miscibility gap and quantitative tie-lines in ternary membranes containing diphytanoyl PC, Biophys. J. 90 (2006) 4428–4436.
[22] A. Pralle, P. Keller, E.L. Florin, K. Simons, J.K.H. Horber, Sphingolipid-cholesterol rafts diffuse as small entities in the plasma membrane of mammalian cells, J. Cell Biol. 148 (2000) 997–1007.
[23] T. Baumgart, G. Hunt, E.R. Farkas, W.W. Webb, G.W. Feigenson, Fluorescence probe partitioning between L-o/L-d phases in lipid membranes, BBA-Biomembranes 1768 (2007) 2182–2194.
[24] V. Kiessling, C. Wan, L.K. Tamm, Domain coupling in asymmetric lipid bilayers, BBA-Biomembranes 1788 (2009) 64–71.
[25] J. Ashcraft, S. Keller, Miscibility phase behavior of GUV membranes containing ternary mixtures of PS lipids, PC lipids, and cholesterol, Biophys. J. 96 (2009) 160a–161a.
[26] H.J. Galla, E. Sackmann, Chemically induced lipid phase separation in model membranes containing charged lipids: a spin label study, BBA-Biomembranes 401 (1975) 509–529.
[27] W. Hartmann, H.J. Galla, E. Sackmann, Direct evidence of charge-induced lipid domain structure in model membranes, FEBS Lett. 78 (1977) 169–172.
[28] M.F. Schneider, D. Marsh, W. Jahn, B. Kloesgen, T. Heimburg, Network formation of lipid membranes: triggering structural transitions by chain melting, Proc. Natl. Acad. Sci. U. S. A. 96 (1999) 14312–14317.
[29] K.A. Riske, L.Q. Amaral, M.T. Lamy, Extensive bilayer perforation coupled with the phase transition region of an anionic phospholipid, Langmuir 25 (2009) 10083–10091.
[30] A. Watts, K. Harlos, W. Maschke, D. Marsh, Control of structure and fluidity of phosphatidylglycerol bilayers by pH titration, Biochim. Biophys. Acta 510 (1978) 63–74.
[31] E.J. Findlay, P.G. Barton, Phase behavior of synthetic phosphatidylglycerols and binary-mixtures with phosphatidylcholines in presence and absence of calcium-ions, Biochemistry 17 (1978) 2400–2405.
[32] K. Akashi, H. Miyata, H. Itoh, K. Kinosita, Preparation of giant liposomes in physiological conditions and their characterization under an optical microscope, Biophys. J. 71 (1996) 3242–3250.
[33] L. Li, J.X. Cheng, Coexisting stripe- and patch-shaped domains in giant unilamellar vesicles, Biochemistry 45 (2006) 11819–11826.
[34] A. Filippov, G. Orädd, G. Lindblom, Effect of NaCl and $CaCl_2$ on the lateral diffusion of zwitterionic and anionic lipids in bilayers, Chem. Phys. Lipids 159 (2009) 81–87.
[35] C.G. Sinn, M. Antonietti, R. Dimova, Binding of calcium to phosphatidylcholine-phosphatidylserine membranes, Colloids Surf., A-Physicochem. Eng. Asp. 282 (2006) 410–419.
[36] D. Uhrikova, N. Kucerka, J. Teixeira, V. Gordeliy, P. Balgavy, Structural changes in dipalmitoylphosphatidylcholine bilayer promoted by Ca^{2+} ions: a small-angle neutron scattering study, Chem. Phys. Lipids 155 (2008) 80–89.
[37] J. Mattai, H. Hauser, R.A. Demel, G.G. Shipley, Interactions of metal-ions with phosphatidylserine bilayer-membranes — effect of hydrocarbon chain unsaturation, Biochemistry 28 (1989) 2322–2330.
[38] P.T. Vernier, M.J. Ziegler, R. Dimova, Calcium binding and head group dipole angle in phosphatidylserine–phosphatidylcholine bilayers, Langmuir 25 (2009) 1020–1027.
[39] A. Lau, A. Mclaughlin, S. Mclaughlin, The adsorption of divalent-cations to phosphatidylglycerol bilayer-membranes, Biochim. Biophys. Acta 645 (1981) 279–292.
[40] J. Marra, J. Israelachvili, Direct measurements of forces between phosphatidylcholine and phosphatidylethanolamine bilayers in aqueous-electrolyte solutions, Biochemistry 24 (1985) 4608–4618.
[41] K. Akashi, H. Miyata, H. Itoh, K. Kinosita, Formation of giant liposomes promoted by divalent cations: critical role of electrostatic repulsion, Biophys. J. 74 (1998) 2973–2982.
[42] I. Koltover, T. Salditt, J.O. Radler, C.R. Safinya, An inverted hexagonal phase of cationic liposome–DNA complexes related to DNA release and delivery, Science 281 (1998) 78–81.
[43] Y.H. Xu, F.C. Szoka, Mechanism of DNA release from cationic liposome/DNA complexes used in cell transfection, Biochemistry 35 (1996) 5616–5623.
[44] R.B. Campbell, S.V. Balasubramanian, R.M. Straubinger, Phospholipid–cationic lipid interactions: influences on membrane and vesicle properties, BBA-Biomembranes 1512 (2001) 27–39.
[45] S. Cinelli, G. Onori, S. Zuzzi, F. Bordi, C. Cametti, S. Sennato, F. Bordi, C. Cametti, S. Sennato, M. Diociaiuti, Properties of mixed DOTAP-DPPC bilayer membranes as reported by differential scanning calorimetry and dynamic light scattering measurements, J. Phys. Chem. B 111 (2007) 10032–10039.
[46] L. Stamatatos, R. Leventis, M.J. Zuckermann, J.R. Silvius, Interactions of cationic lipid vesicles with negatively charged phospholipid-vesicles and biological-membranes, Biochemistry 27 (1988) 3917–3925.
[47] K. Anzai, M. Masumi, K. Kawasaki, Y. Kirino, Frequent fusion of liposomes to a positively charged planar bilayer without calcium-ions, J. Biochem. (Tokyo) 114 (1993) 487–491.
[48] C.M. Franzin, P.M. Macdonald, Detection and quantification of asymmetric lipid vesicle fusion using deuterium NMR, Biochemistry 36 (1997) 2360–2370.
[49] M.I. Angelova, D.S. Dimitrov, Liposome electroformation, Faraday Discuss. 81 (1986) 303–311.
[50] A.G. Ayuyan, F.S. Cohen, Lipid peroxides promote large rafts: effects of excitation of probes in fluorescence microscopy and electrochemical reactions during vesicle formation, Biophys. J. 91 (2006) 2172–2183.
[51] J. Zhao, J. Wu, H.L. Shao, F. Kong, N. Jain, G. Hunt, G. Feigenson, Phase studies of model biomembranes: macroscopic coexistence of L alpha plus L beta, with light-induced coexistence of L alpha plus Lo Phases, BBA-Biomembranes 1768 (2007) 2777–2786.
[52] L.A. Bagatolli, E. Gratton, A correlation between lipid domain shape and binary phospholipid mixture composition in free standing bilayers: a two-photon fluorescence microscopy study, Biophys. J. 79 (2000) 434–447.
[53] S.L. Veatch, S.L. Keller, Organization in lipid membranes containing cholesterol, Phys. Rev. Lett. 89 (2002) 4.
[54] T. Baumgart, S. Das, W.W. Webb, J.T. Jenkins, Membrane elasticity in giant vesicles with fluid phase coexistence, Biophys. J. 89 (2005) 1067–1080.
[55] D.A. Mannock, T.J. McIntosh, X. Jiang, D.F. Covey, R.N. McElhaney, Effects of natural and enantiomeric cholesterol on the thermotropic phase behavior and structure of egg sphingomyelin bilayer membranes, Biophys. J. 84 (2003) 1038–1046.

[56] B. Ramstedt, J.P. Slotte, Comparison of the biophysical properties of racemic and d-erythro-N-acyl sphingomyelins, Biophys. J. 77 (1999) 1498–1506.
[57] J.Y. Huang, G.W. Feigenson, A microscopic interaction model of maximum solubility of cholesterol in lipid bilayers, Biophys. J. 76 (1999) 2142–2157.
[58] J.Y. Huang, J.T. Buboltz, G.W. Feigenson, Maximum solubility of cholesterol in phosphatidylcholine and phosphatidylethanolamine bilayers, BBA-Biomembranes 1417 (1999) 89–100.
[59] A. Wisniewska, W.K. Subczynski, The liquid-ordered phase in sphingomyelincholesterol membranes as detected by the discrimination by oxygen transport (DOT) method, Cell. Mol. Biol. Lett. 13 (2008) 430–451.
[60] T.N. Estep, D.B. Mountcastle, Y. Barenholz, R.L. Biltonen, T.E. Thompson, Thermal-behavior of synthetic sphingomyelin-cholesterol dispersions, Biochemistry 18 (1979) 2112–2117.
[61] P.R. Maulik, G.G. Shipley, N-palmitoyl sphingomyelin bilayers: structure and interactions with cholesterol and dipalmitoylphosphatidylcholine, Biochemistry 35 (1996) 8025–8034.
[62] R.F.M. de Almeida, A. Fedorov, M. Prieto, Sphingomyelin/phosphatidylcholine/cholesterol phase diagram: boundaries and composition of lipid rafts, Biophys. J. 85 (2003) 2406–2416.
[63] S.L. Veatch, S.L. Keller, Miscibility phase diagrams of giant vesicles containing sphingomyelin, Phys. Rev. Lett. 94 (2005) 148101.
[64] T.H. Huang, C.W.B. Lee, S.K. Dasgupta, A. Blume, R.G. Griffin, A C-13 and H-2 nuclear-magnetic-resonance study of phosphatidylcholine cholesterol interactions — characterization of liquid-gel phases, Biochemistry 32 (1993) 13277–13287.
[65] M.M.A.E. Claessens, F.A.M. Leermakers, F.A. Hoekstra, M.A.C. Stuart, Osmotic shrinkage and reswelling of giant vesicles composed of dioleoylphosphatidylglycerol and cholesterol, BBA-Biomembranes 1778 (2008) 890–895.
[66] S.L. Veatch, S.L. Keller, Seeing spots: complex phase behavior in simple membranes, BBA-Mol. Cell Res. 1746 (2005) 172–185.
[67] A. Filippov, G. Oradd, G. Lindblom, Sphingomyelin structure influences the lateral diffusion and raft formation in lipid bilayers, Biophys. J. 90 (2006) 2086–2092.
[68] F.M. Goni, A. Alonso, L.A. Bagatolli, R.E. Brown, D. Marsh, M. Prieto, J.L. Thewalt, Phase diagrams of lipid mixtures relevant to the study of membrane rafts, BBA-Mol. Cell Biol. Lipids 1781 (2008) 665–684.
[69] S.L. Veatch, S.L. Keller, A closer look at the canonical 'raft mixture' in model membrane studies, Biophys. J. 84 (2003) 725–726.
[70] R. Lipowsky, R. Dimova, Domains in membranes and vesicles, J. Phys.: Condens. Matter 15 (2003) S31–S45.
[71] A. Roux, D. Cuvelier, P. Nassoy, J. Prost, P. Bassereau, B. Goud, Role of curvature and phase transition in lipid sorting and fission of membrane tubules, EMBO J. 24 (2005) 1537–1545.
[72] A. Tian, T. Baumgart, Sorting of lipids and proteins in membrane curvature gradients, Biophys. J. 96 (2009) 2676–2688.
[73] B. Sorre, A. Callan-Jones, J.B. Manneville, P. Nassoy, J.F. Joanny, J. Prost, B. Goud, P. Bassereau, Curvature-driven lipid sorting needs proximity to a demixing point and is aided by proteins, Proc. Natl. Acad. Sci. U. S. A. 106 (2009) 5622–5626.
[74] K.A. Riske, H.G. Dobereiner, M.T. Lamy-Freund, Comment on "Gel–fluid transition in dilute versus concentrated DMPG aqueous dispersions", J. Phys. Chem. B 107 (2003) 5391–5392.
[75] K.A. Riske, R.L. Knorr, R. Dimova, Bursting of charged multicomponent vesicles subjected to electric pulses, Soft Matter 5 (2009) 1983–1986.
[76] S. Mittler-Neher, W. Knoll, Ca^{2+}-induced lateral phase-separation in black lipid-membranes and its coupling to the ion translocation by gramicidin, Biochim. Biophys. Acta 1152 (1993) 259–269.
[77] J.M. Boggs, G. Rangaraj, Investigation of the metastable phase-behavior of phosphatidylglycerol with divalent-cations by calorimetry and manganese ion binding measurements, Biochemistry 22 (1983) 5425–5435.
[78] S. Ohki, A mechanism of divalent ion-induced phosphatidylserine membrane-fusion, Biochim. Biophys. Acta 689 (1982) 1–11.
[79] S. Ohki, H. Ohshima, Divalent cation-induced phosphatidic-acid membrane-fusion — effect of ion binding and membrane-surface tension, Biochim. Biophys. Acta 812 (1985) 147–154.
[80] R.M. Fernandez, K.A. Riske, L.Q. Amaral, R. Itri, M.T. Lamy, Influence of salt on the structure of DMPG studied by SAXS and optical microscopy, BBA-Biomembranes 1778 (2008) 907–916.
[81] V.D. Gordon, M. Deserno, C.M.J. Andrew, S.U. Egelhaaf, W.C.K. Poon, Adhesion promotes phase separation in mixed-lipid membranes, Epl 84 (2008).
[82] J.C. Shillcock, R. Lipowsky, Tension-induced fusion of bilayer membranes and vesicles, Nat. Mater. 4 (2005) 225–228.
[83] R.N.A.H. Lewis, R.N. McElhaney, Surface charge markedly attenuates the nonlamellar phase-forming propensities of lipid bilayer membranes: calorimetric and P-31-nuclear magnetic resonance studies of mixtures of cationic, anionic, and zwitterionic lipids, Biophys. J. 79 (2000) 1455–1464.
[84] T.S. Ursell, W.S. Klug, R. Phillips, Morphology and interaction between lipid domains, Proc. Natl. Acad. Sci. 106 (2009) 13301–13306.
[85] D. Lingwood, J. Ries, P. Schwille, K. Simons, Plasma membranes are poised for activation of raft phase coalescence at physiological temperature, Proc. Natl. Acad. Sci. U. S. A. 105 (2008) 10005–10010.